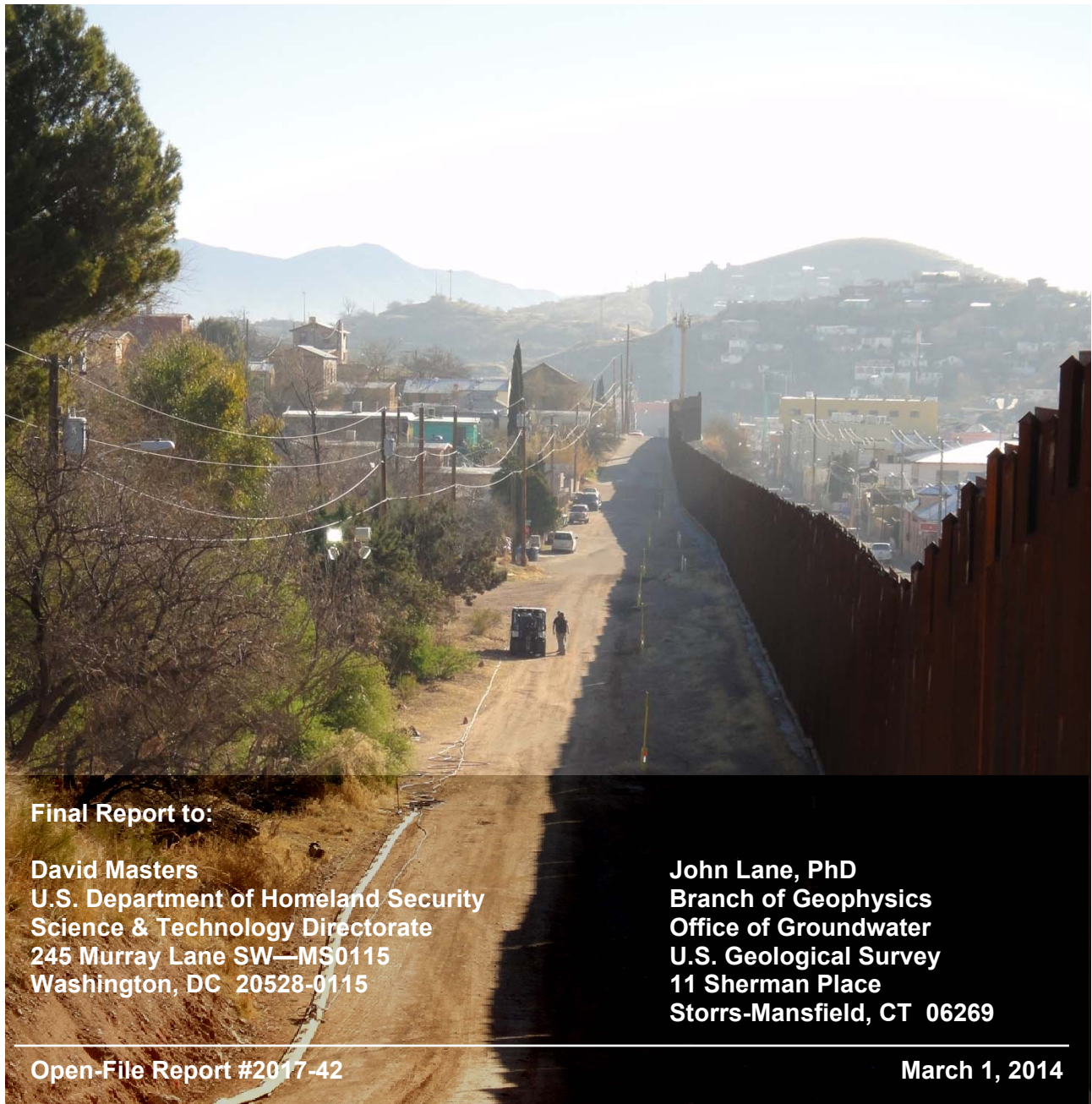


Final Report: Seismic Analysis at Strategic Border Sites Nog_N2 (DTRA N4a)

Richard D. Miller, J. Tyler Schwenk, Julian Ivanov,
Shelby L. Peterie, J. Jordan Nolan, Brett Wedel,
Ryan Nelson, Brett Bennett, and Joe Anderson

Kansas Geological Survey
1930 Constant Avenue
Lawrence, KS 66047



Final Report to:

David Masters
U.S. Department of Homeland Security
Science & Technology Directorate
245 Murray Lane SW—MS0115
Washington, DC 20528-0115

John Lane, PhD
Branch of Geophysics
Office of Groundwater
U.S. Geological Survey
11 Sherman Place
Storrs-Mansfield, CT 06269

The Kansas Geological Survey makes no warranty or representation, either express or implied, with regard to the data, documentation, or interpretations or decisions based on the use of this data including the quality, performance, merchantability, or fitness for a particular purpose. Under no circumstances shall the Kansas Geological Survey be liable for damages of any kind, including direct, indirect, special, incidental, punitive, or consequential damages in connection with or arising out of the existence, furnishing, failure to furnish, or use of or inability to use any of the database or documentation whether as a result of contract, negligence, strict liability, or otherwise. This study was conducted in complete compliance with ASTM Guide D7128-05. All data, interpretations, and opinions expressed or implied in this report and associated study are reasonably accurate and in accordance with generally accepted scientific standards.

Final Report: Seismic Analysis at Strategic Border Sites Nog_N2 (DTRA N4a)

Summary

The Kansas Geological Survey acquired borehole and surface seismic data at 15 DHS sites near the US-Mexico border. Surface seismic data were processed using multi-channel analysis of surface waves (MASW), refraction tomography, and surface wave inversion to obtain 2-D profiles of shear-wave velocity (V_s), compressional-wave velocity (V_p), and seismic quality factor (Q_s and Q_p) for the near surface. Downhole data were processed to obtain downhole V_s , V_p , Q_s , and Q_p . This report contains final processing and results for Nog_N2 (DTRA N4a).

Data Acquisition

One line of seismic data (~175 m) was acquired on February 26, 2013, at Nog_N2 (DTRA N4a) coincident with the USGS ERT profile (Figure 1). The system of sources and receivers, collectively, is the Active Seismic Imaging (ASI) system developed by and fabricated at the Kansas Geological Survey (Figure 2). Seismic sources were an accelerated weight drop for surface wave and long-offset compressional energy, sledge hammer and steel plate for near-offset compressional-wave energy, and sledge hammer and shear block for shear-wave energy. Seismic receivers were located in a towed 144-channel 3-component (3-C) land streamer with 48 stations separated by 1.2 m. Receivers were single 4.5 Hz and 40 Hz vertical geophones and two 14.5 Hz horizontal (SV orientation) geophones (Figure 3). Seismographs were a Geometrics Geode distributed system. The survey was fixed spread with variable 0-85.3 m source offset (Figure 4) to obtain sufficient seismic sampling within the depth of interest. Individual receiver spreads overlapped by one station.

Downhole data were acquired on January 23-24, 2014, approximately 325 m from the center of the surface seismic line, with a 3-C downhole Geostuff geophone (Figure 5). Receivers were located between depths of approximately 2.3 m and 45.7 m at approximately 0.75 m intervals (Figure 6). A repeatable shear and compressional 9 kg hammer source (Figure 7), developed and fabricated at the Kansas Geological Survey, was located at 3 m from the borehole. A 2.7 kg sledge hammer and steel plate were located at 22.9 m from the borehole.

For both the surface and downhole seismic surveys, multiple shots were acquired and recorded separately for each unique shot/receiver configuration and stacked during processing to minimize ambient noise (Figure 8) and increase the signal-to-noise ratio.



Figure 1: Aerial photo of Nog_N2 (DTRA N4a) and location of the active seismic line.



Figure 2: ASI and 144-channel 3-C land streamer, detached.

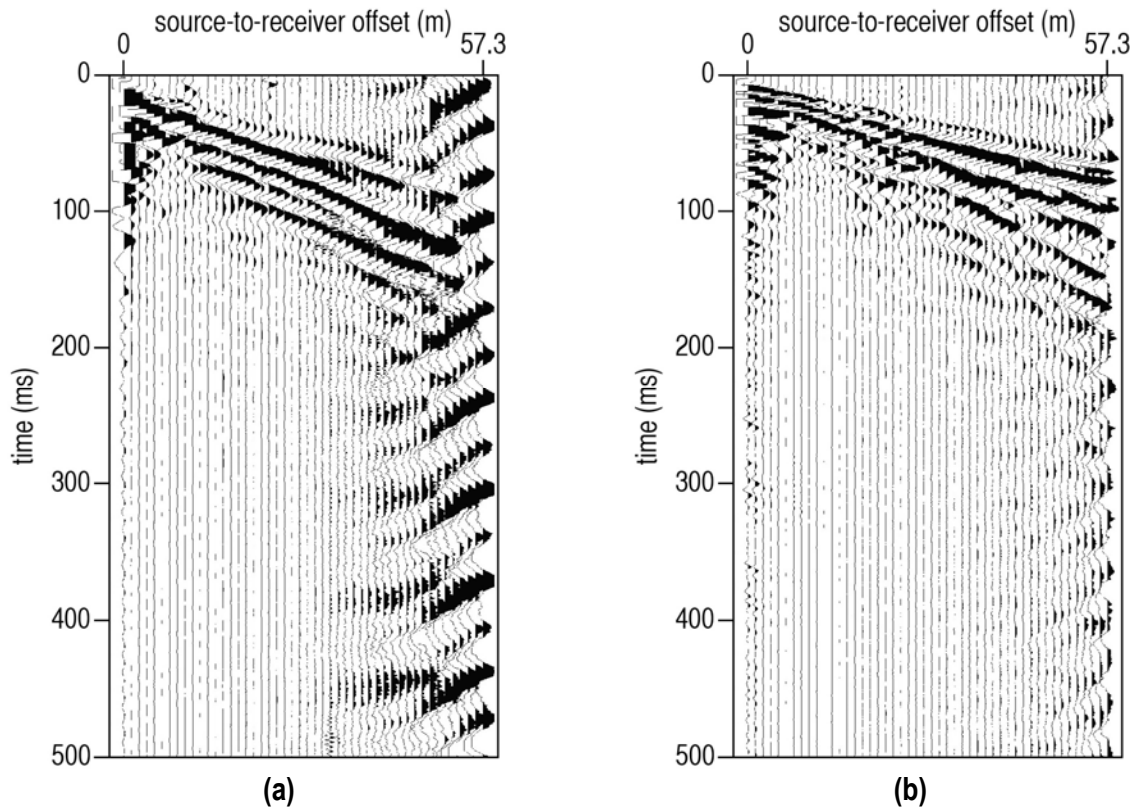


Figure 3: Representative off-end shot gathers at Nog_N2 (DTRA N4a). (a) Sledge hammer and shear block source recorded with shear 14.5 Hz geophones, SV orientation. (b) Weight-drop source recorded with vertical 40 Hz geophones.

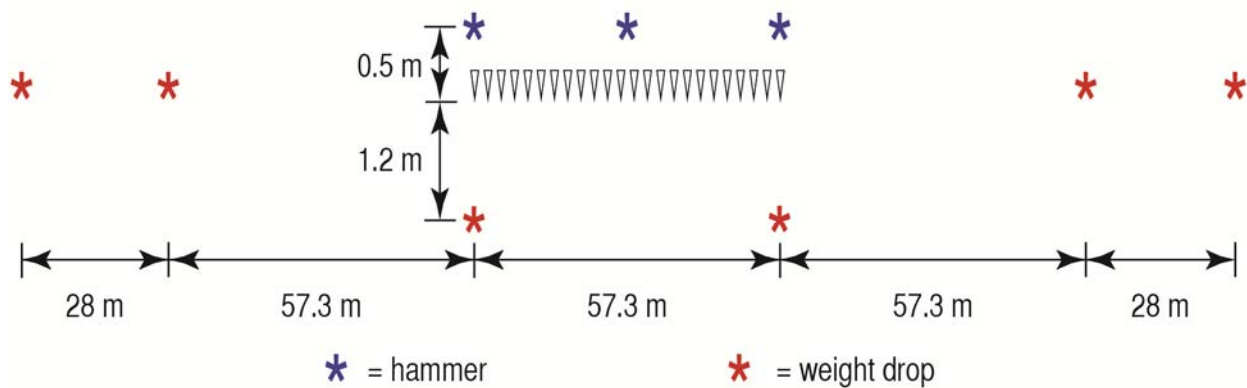


figure not to scale

Figure 4: Diagram indicating all shot point locations relative to a single receiver spread. The receiver spread consisted of 48 stations separated by 1.2 m.

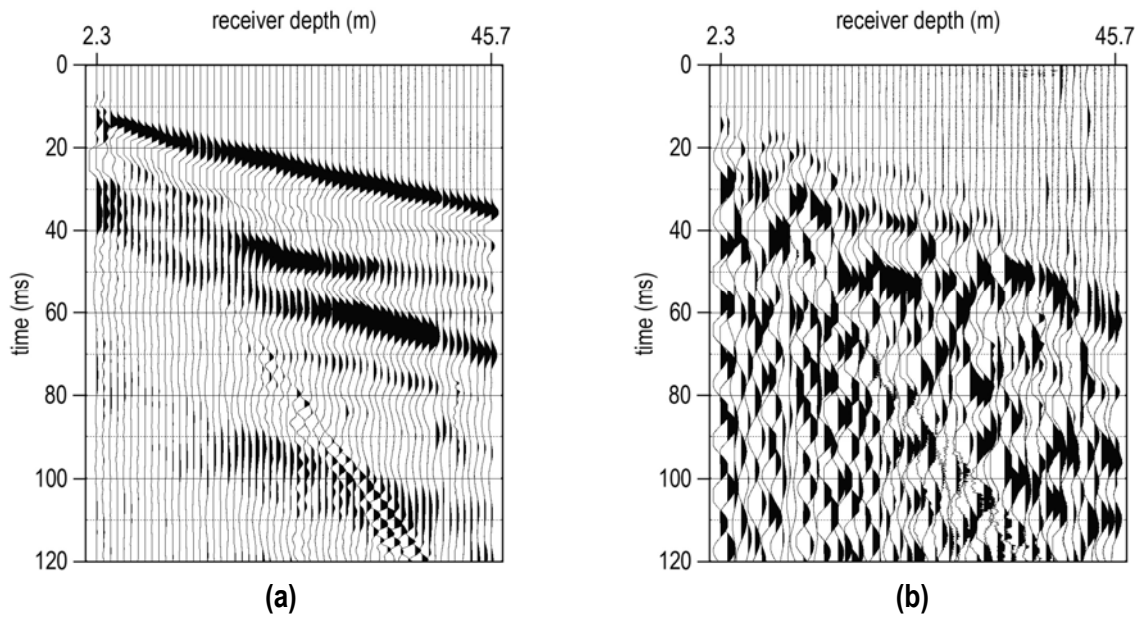


Figure 5: Representative unprocessed downhole (a) vertical, and (b) shear records at Nog_N2 (DTRA N4a).

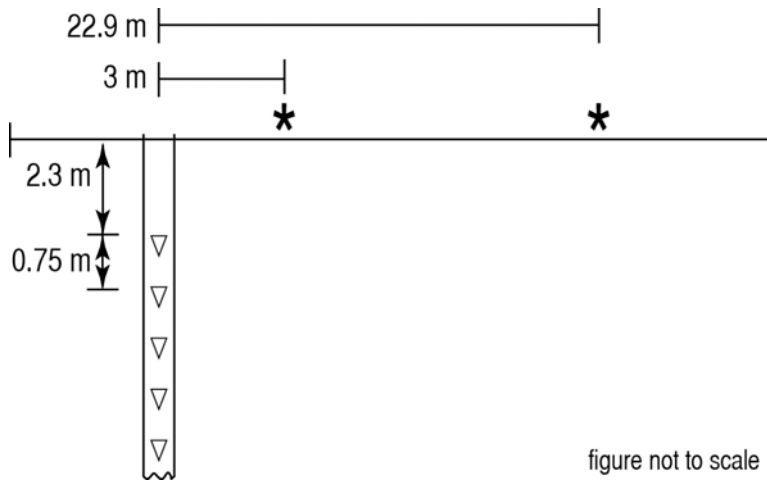


Figure 6: Downhole seismic field layout.



Figure 7: Downhole seismic acquisition at Nog_N2 (DTRA N4a).

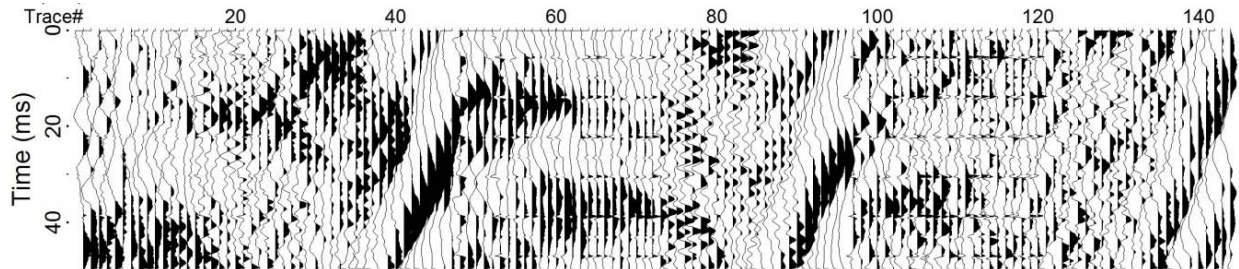


Figure 8. Representative ambient noise recorded at Nog_N2 (DTRA N4a). Traces 1-48 represent the 4.5 Hz geophones, 49-96 represent the shear geophones, and 97-144 represent the 40 Hz geophones.

Data Processing

Multichannel-analysis of surface waves (MASW) was used to analyze dispersive Rayleigh-wave energy and estimate shear-wave velocity (V_s). Fundamental-mode energy was interpreted and inverted using a weighted, damped least-squares approach (Xia et al., 1999), resulting in a 2-D V_s profile. Average and interval downhole compressional-wave velocity (V_p) and V_s were calculated using the arrival time of the direct P-wave and S-wave, respectively, and pathlength from the seismic source to each receiver depth. Refraction tomography with 1.2 x 1.2 m cell size was used to estimate V_s and V_p . Joint-analysis of refractions and surface waves (JARS, Ivanov et al., 2010) was used to constrain the non-uniqueness inherently involved in refraction inversion, resulting in physically realistic 2-D V_s and V_p profiles. Shear- and compressional-wave seismic quality factors (Q_s and Q_p , respectively) were obtained using a surface wave inversion technique (Xia et al., 2010). Downhole shear records were numerically rotated to orient the recorded shear-wave traces in the vertical (SV) and horizontal (SH) polarization directions (Di Siena et al., 1984). The direct P-waves and S-waves were isolated on compressional and shear records, respectively, and the spectral ratio method was used to estimate Q_p and Q_s for each lithology identified in drilling notes (Tonn, 1991; Hasse and Stewart, 2004). The velocity and quality values calculated from downhole data were used to constrain inversion and improve accuracy of the results obtained using surface seismic methods.

Final Results

MASW

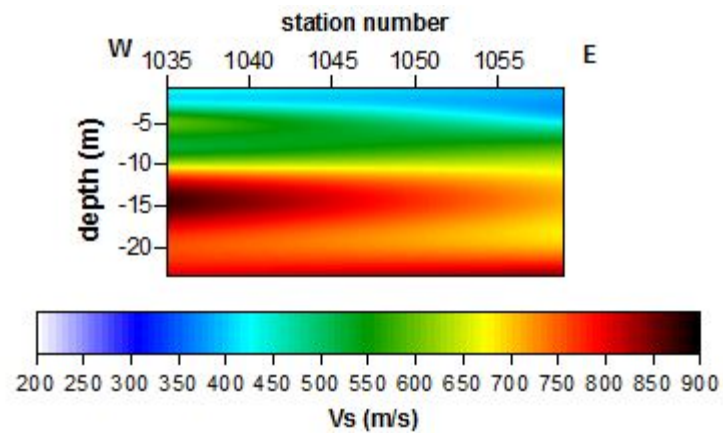


Figure 9: MASW V_s at Nog_N2 (DTRA N4a).

Downhole Vs

The characteristics of the direct wave recorded in the upper 8 m appear to be consistent with wavelet characteristics observed at other sites where grout is poorly bonded to the formation. The apparent large velocity gradient at a depth of 8 m is possibly due to poor quality bond; however, this cannot be confirmed because bond logs were not acquired at this site. The apparent downhole shear-wave interval velocity is faster than expected for the lithology described on the boring logs. This is most likely due to a mode conversion, possibly at the alluvium/sandstone interface.

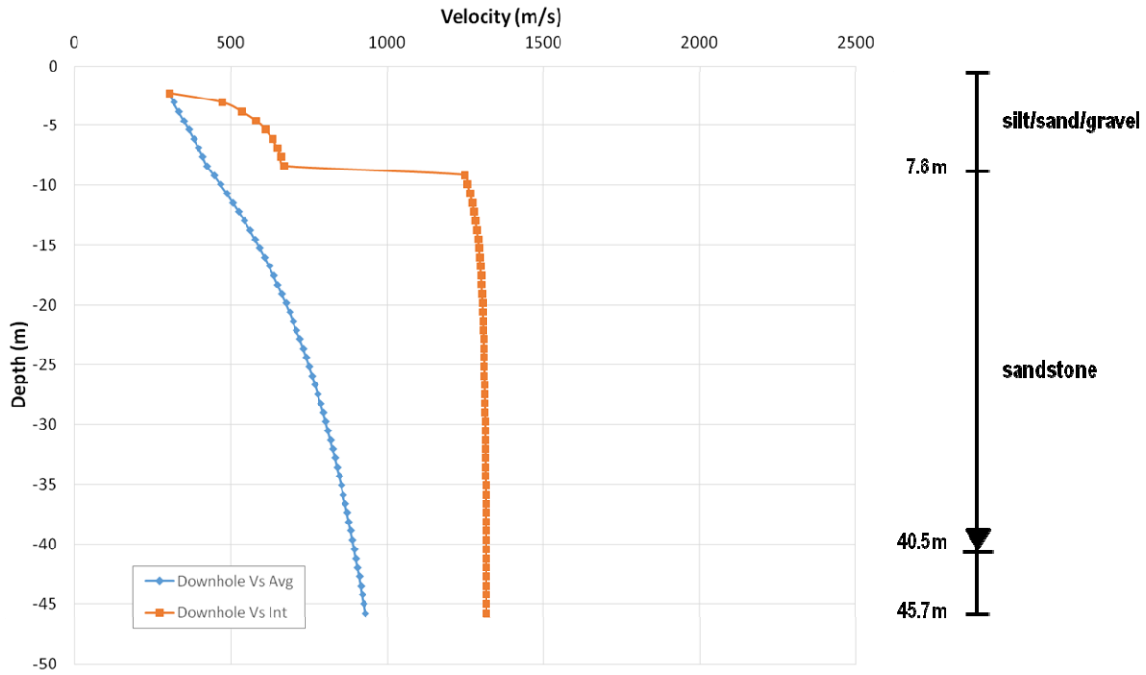


Figure 10: Downhole Vs profile at Nog_N2 (DTRA N4a).

Downhole V_p

The characteristics of the direct wave recorded in the upper 8 m appear to be consistent with wavelet characteristics observed at other sites where grout is poorly bonded to the formation. The apparent large velocity gradient at a depth of 8 m is possibly due to poor quality bond; however, this cannot be confirmed because bond logs were not acquired at this site.

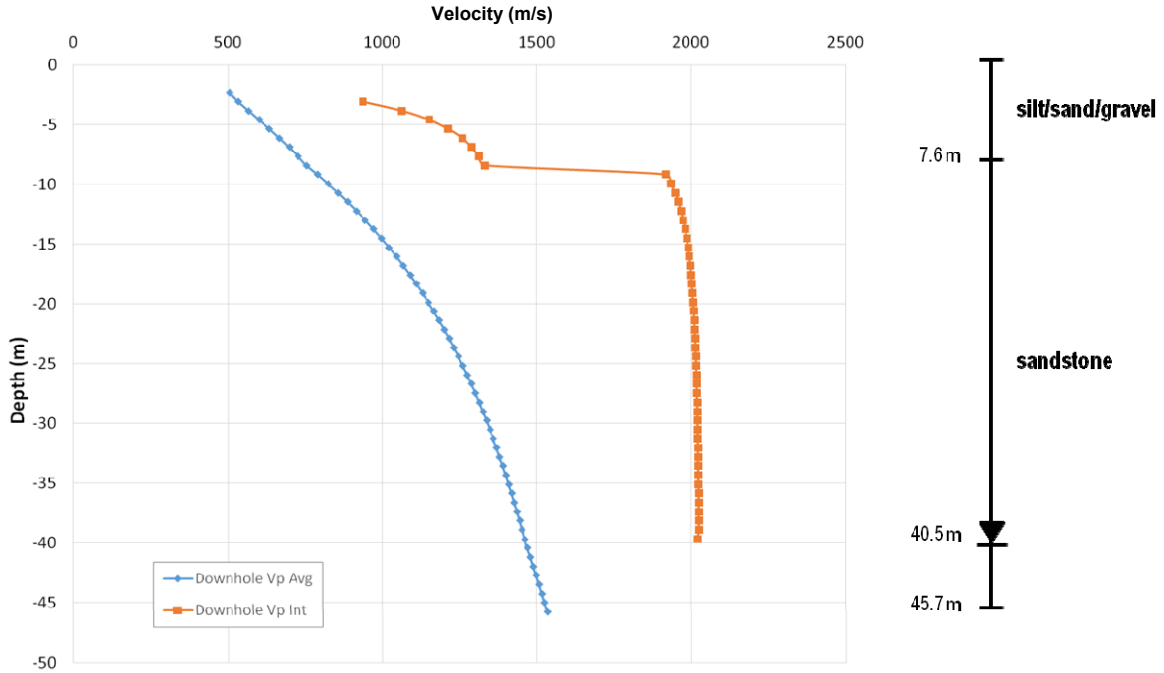


Figure 11: Downhole V_p profile at Nog_N2 (DTRA N4a).

Vs Tomography

A smoothed version of the final MASW Vs profile was used as the initial model. Picked first arrival times used for preliminary processing were reviewed to confirm their accuracy and used for final processing.

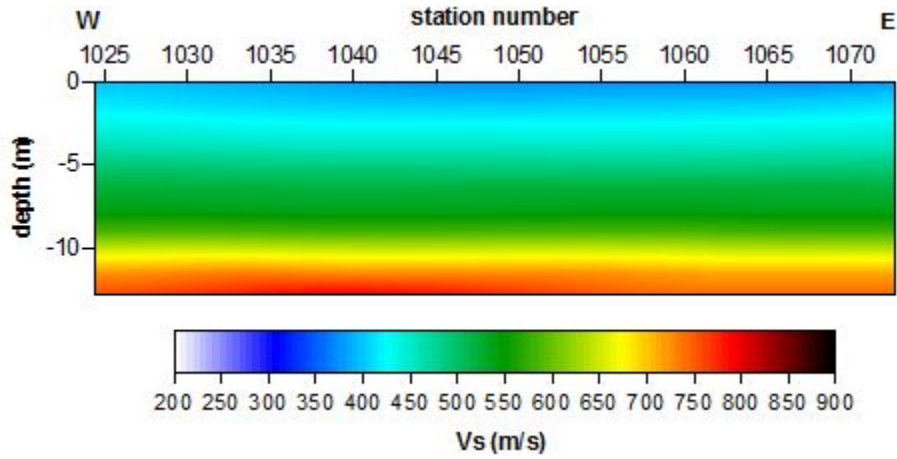


Figure 12: Vs tomography at Nog_N2 (DTRA N4a).

V_p Tomography

Scaled, smoothed MASW velocities were a very accurate initial model at lower station numbers located on a hillside. Borehole P-wave velocities were a very accurate initial model at higher station numbers located at the base of the hill. Therefore, an initial model was generated by interpolating between scaled, smoothed MASW velocities at low stations and the downhole interval V_p at high stations. Picked first arrival times used for preliminary processing were reviewed to confirm their accuracy and used for final processing.

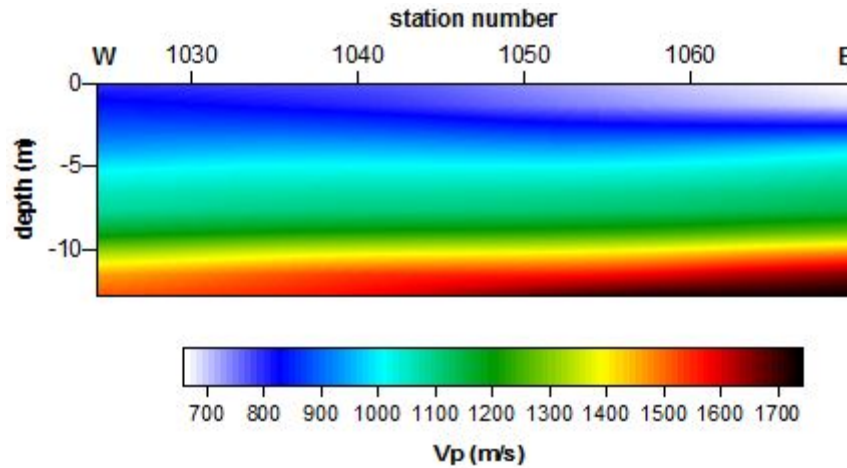


Figure 13: V_p tomography at Nog_N2 (DTRA N4a).

Downhole Q_s

Calculation of Q is highly sensitive to sources of noise (e.g., traffic) during acquisition.

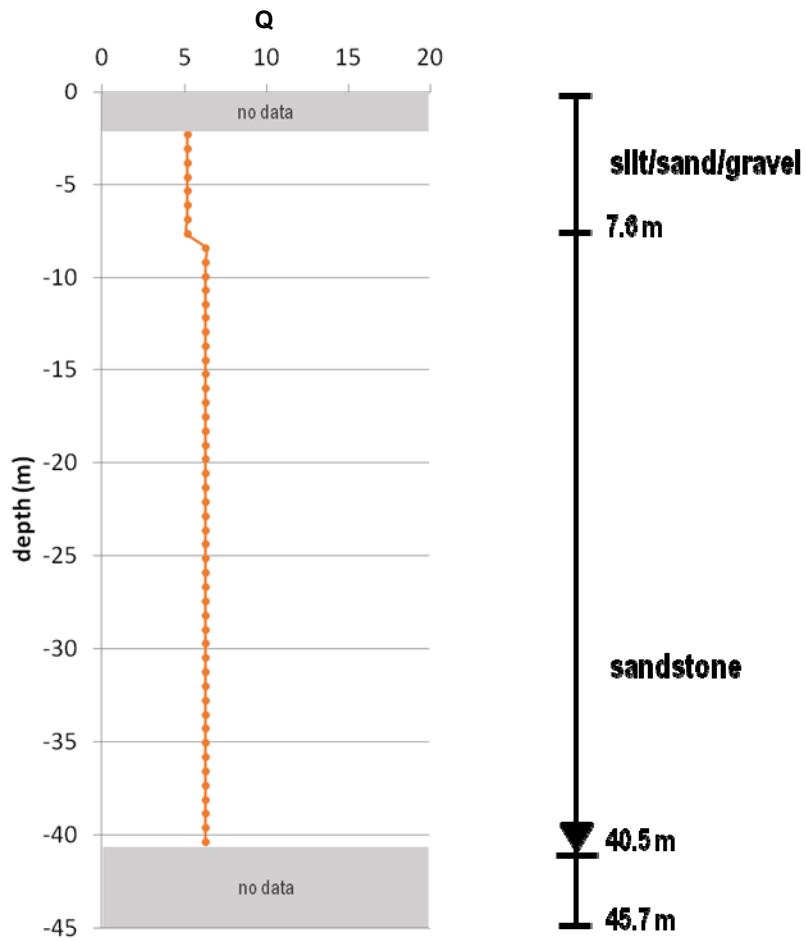


Figure 14: Downhole Q_s profile at Nog_N2 (DTRA N4a).

Downhole Qp

Calculation of Q is highly sensitive to sources of noise (e.g., traffic) during acquisition.

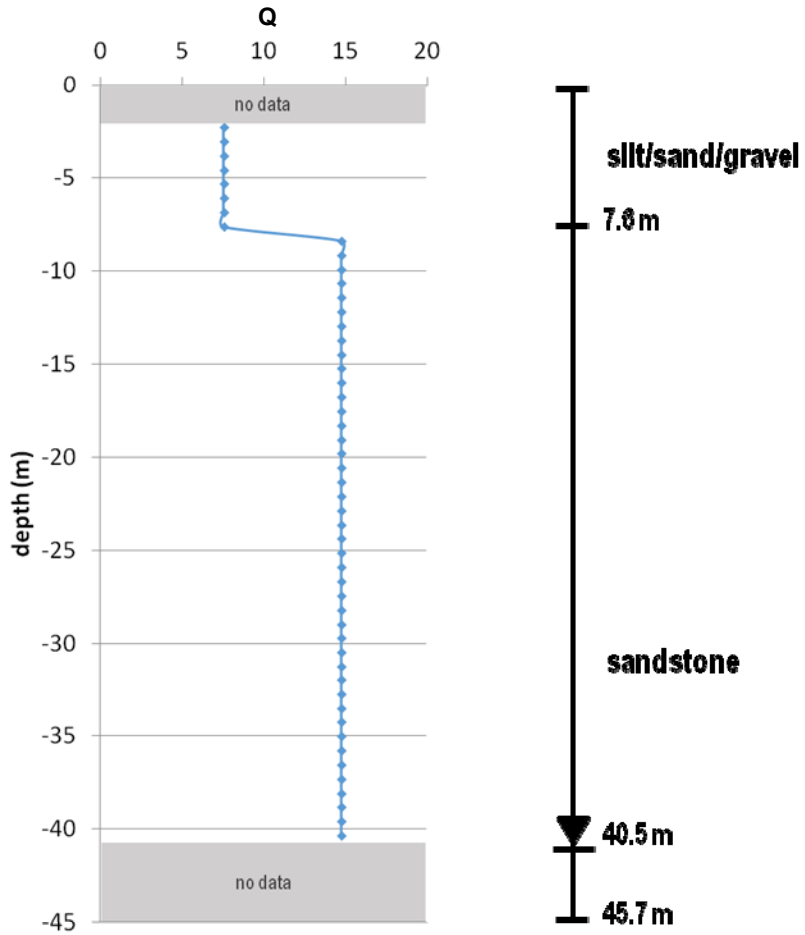


Figure 15: Downhole Qp profile at Nog_N2 (DTRA N4a).

Surface Q_s

Calculation of Q is highly sensitive to sources of noise (e.g., traffic) during acquisition. Due to lack of stability in the inversion, the upper 0-5 m is low confidence.

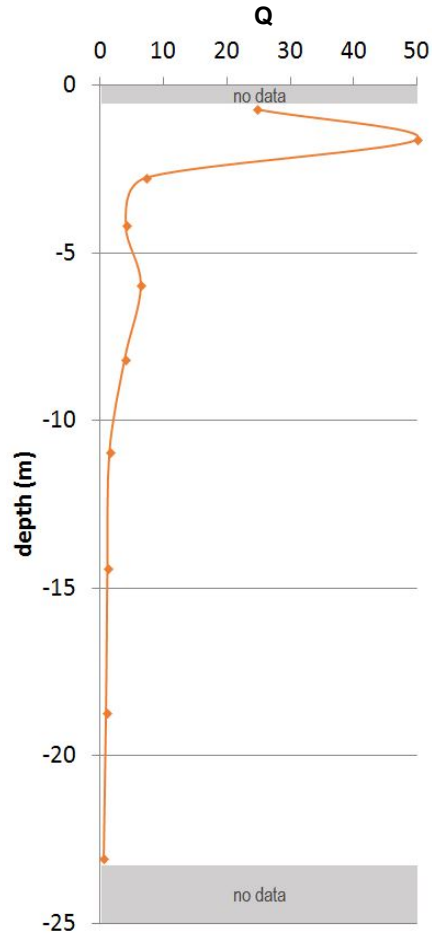


Figure 16: Surface Q_s at Nog_N2 (DTRA N4a).

Surface Q_p

Calculation of Q is highly sensitive to sources of noise (e.g., traffic) during acquisition. Due to lack of stability in the inversion, the upper 0-5 m is low confidence.

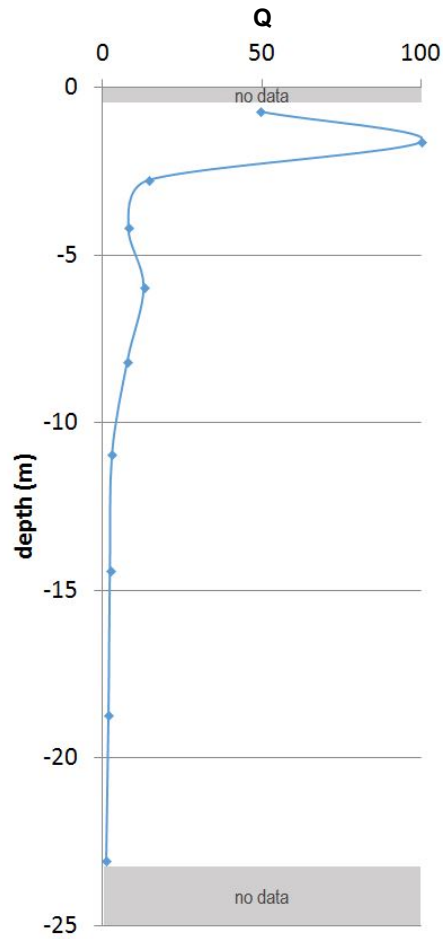


Figure 17: Surface Q_p profiles for at Nog_N2 (DTRA N4a).

Related Materials

Delivered materials include:

1. This report
2. PowerPoint presentation summarizing this report
3. Data files
4. Document explaining the data file format
5. Detailed list of deliverables

References

- Di Siena, J.P., J.E. Gaiser, and D. Corrigan, 1984, Horizontal components and shear wave analysis of three component VSP data, in *Vertical Seismic Profiling, Part B: Advanced Concepts*, pp. 175-235, eds. M.N. Toksöz and R.R. Stewart, Geophysical Press, London.
- Hasse, A.B. and R.R. Stewart, 2004, Attenuation estimates from VSP and log data: SEG expanded abstracts, 2497-2500.
- Ivanov, J., R.D. Miller, J. Xia, J.B. Dunbar, and S. Peterie, 2010, Chapter 20: Refraction non-uniqueness studies at levee sites using the refraction-tomography and JARS methods: in *Advances in Near-Surface Seismology and Ground-Penetrating Radar*, SEG Geophysical Developments Series No. 15, R. D. Miller, J. D. Bradford, and K. Holliger, eds., Society of Exploration Geophysicists, 327-338.
- Tonn, R., 1991, The determination of the seismic quality factor Q from VSP data: A comparison of different computational methods: *Geophysical Prospecting*, **39**, 1-27.
- Xia, J., and R.D. Miller, 2010, Chapter 2: Estimation of near-surface shear-wave velocity and quality factor by inversion of high-frequency Rayleigh waves: in *Advances in Near-Surface Seismology and Ground-Penetrating Radar*, SEG Geophysical Developments Series No. 15, R. D. Miller, J. D. Bradford, and K. Holliger, eds., Society of Exploration Geophysicists, 17-36.
- Xia, J., R.D. Miller, and C. B. Park, 1999, Estimation of near-surface velocity by inversion of Rayleigh waves: *Geophysics*, **64**, 691-700.